Non-invasive Angiographic-based Fractional Flow Reserve: Technical Development, Clinical Implications, and Future Perspectives

Joyce Peper[1, 2#], Michiel L. Bots[3], Tim Leiner[2], Martin J. Swaans[1]
[1]*Department of Cardiology, St. Antonius Hospital, Nieuwegein 3435 CM, The Netherlands*
[2]*Department of Radiology, University Medical Center Utrecht, Utrecht 3508 GA, The Netherlands*
[3]*Julius Center for Health Sciences and Primary Care, University Medical Center Utrecht, Utrecht 3584 CG, The Netherlands*

[Abstract] New non- and less-invasive techniques have been developed to overcome the procedural and operator related burden of the fractional flow reserve (FFR) for the assessment of potentially significant stenosis in the coronary arteries. Virtual FFR-techniques can obviate the need for the additional flow or pressure wires as used for FFR measurements. This review provides an overview of the developments and validation of the virtual FFR-algorithms, states the challenges, discusses the upcoming clinical trials, and postulates the future role of virtual FFR in the clinical practice.
Key words: coronary artery disease; quantitative flow ratio; fractional flow reserve; diagnostic accuracy; physiology guided percutaneous coronary intervention

Invasive coronary angiography (ICA) is the most often used diagnostic test for the assessment of significant obstructive stenosis. Yet the relationship between anatomical significant stenosis and the physiological reduction of the myocardial blood flow is weak[1]. Moreover, the assessment of the stenosis would depend on the visual interpretation of the cardiologist, which could be challenging in intermediate lesions. Fractional flow reserve (FFR), a physiological test, serves as a surrogate for myocardial blood flow test since direct coronary blood flow measurements are difficult to perform. FFR is defined as the mean distal coronary pressure measured with the pressure wire, divided by the mean proximal coronary or aortic pressure, measured with a guide catheter during maximal hyperemia, and presented as a percentage. An hemodynamical reduction is defined as a 20% reduction of the FFR (FFR $\leq$0.80)[2]. It can be used in addition to an ICA to assess the hemodynamical impact of a stenosis and serve as a guiding tool to identify patients who might benefit from revascularization. Furthermore, FFR-guided coronary intervention would improve the clinical outcomes, quality of life, and reduce stent implantations and thereby costs compared to an ICA-guided strategy[2]. Nevertheless, it has been used in less than 19% of patients due to the challenges in the logistical aspects in both the procedural and operator related factors[3, 4]. The reasons for not using FFR can be found in its availability, the additional time needed for the set up and measurement compared to an ICA, the financial costs of the FFR pressure wire and adenosine infusion, contraindications for FFR, and the increased risk of complications caused by the invasiveness of the measurement since the wire would need to pass the stenosis[5, 6].

New non- and less-invasive techniques have also been developed to overcome the burden and limitations of FFR. They can obviate the need for the additional flow or pressure wires as used for the FFR measurements. Therefore, this review provides an overview of the development and validation of different virtual FFR algorithms, and we discuss the technical and implementation challenges, ongoing and upcoming clinical trials, and the expected role of virtual FFR in the clinical practice. The focus of this review is on angiography-based FFR-techniques, whereas computed tomography (CT) derived FFR and optical coherence tomography derived FFR are beyond the scope.

1 COMPUTATIONAL FLUID DYNAMICS

Virtual FFR software mainly uses estimations based on the principles of fluid dynamics, a mathematical method to model and understand the (blood) flow. Using images of the coronary arteries, these calculations could be used to create *in silico* (simulated by computer) models representing the hemodynamic situation of the cardiovascular system. This would allow studying the blood flow in the coronary arteries non-invasively and help to assess the hemodynamic impact of a stenosis. Fluid

#Corresponding author, E-mail: j.peper@antoniusziekenhuis.nl

dynamics applied to models of the coronary arteries have also been comprehensively reviewed[7]. In brief, construction of a fluid dynamics model (fig. 1) would consist of the four steps.

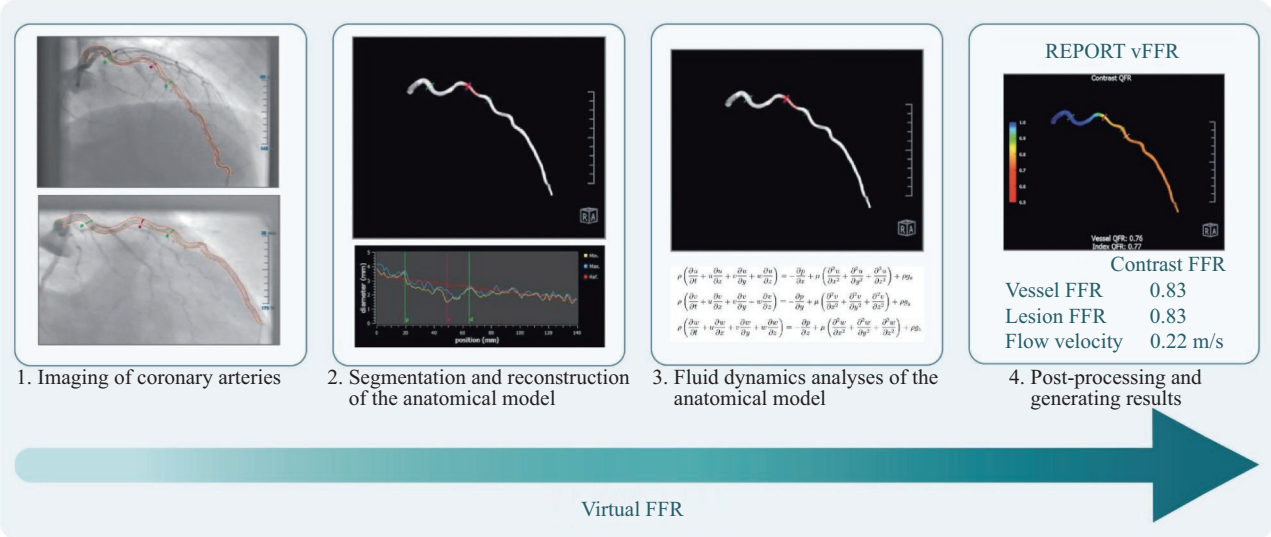

Fig. 1 Overview of the four steps of computing a virtual FFR
1. imaging of the coronary arteries in two views using invasive coronary angiography; 2. segmentation of the coronary artery of interest and reconstruction of the anatomical model; 3. fluid dynamics models based on the analyses to simulate the flow; 4. post-processing of the data and generating a report for clinical practice

1.1 Imaging of the Coronary Arteries

Different imaging modalities, as invasive coronary angiography, could be used to visualize the coronary arteries. The imaging quality would be crucial since sufficient anatomical and physiological details would need to be extracted to enable further steps in the modeling process.

1.2 Reconstruction and Segmentation of the Anatomical Model

The next step would include the transition from the acquired images to the reconstruction of an anatomical model of the coronary vessels. Three-dimensional quantitative coronary angiography (3D-QCA) is the most frequently used approach to convert the images acquired using invasive coronary angiography into *in silico* geometries, e.g., concatenated cylinders representing the coronary vessels[8, 9]. In general, two angiographic views of at least 25° apart would be used and selected based on the least foreshortening of the stenosis with a minimum overlap between the main vessels and side branches. The vessels' contours would be semi-automatically detected using an anatomical landmark in both views to construct a 3D model. In addition, proximal and distal points would need to be appointed to indicate the part of the vessel that would be evaluated. Manual additions of the vessel contours could also be made if needed.

The anatomical model would be converted into smaller structures, so-called discretization, or meshing. A mesh is the smallest unit in which the flow would be calculated, which would be conducted individually by solving the equations for the flow estimation. All the connected meshes with a combined approach would flow in the coronary vessels. Different context-specific methods and settings could be applied for meshing and the level of refinement balancing the accuracy and numerical stability of the analysis. The mesh would need to be sophisticated enough to capture the physiological situation but should avoid excessive computations to limit the solution time.

1.3 Flow Analyses

In addition to the mesh, several boundary conditions would need to be set to enable the flow analysis. These boundary conditions would define the hemodynamic or structural conditions at the inlets (i.e., aorta blood flow), outlets (i.e., coronary microvascular resistance), and coronary artery walls. The conditions would be set based on the patient-specific or population data, physical models, or assumptions.

Besides the boundary conditions, other properties, such as blood density, blood viscosity, and the initial conditions of the model would need to be set in the developmental phase of the algorithm to estimate the blood flow. There would be two main strategies to estimate the coronary flow: 1) computational fluid dynamics (CFD) calculations that would apply the Navier-Stokes equations, and 2) empirical fluid dynamic equations[10]. The CFD models would use the principle of the conservation of mass and momentum to estimate the flow in all individual meshes. The complex geometry of the coronary arteries would require specialized software to approximate the solution, which would require excessive computations and would be time-consuming. Alternatively, empirical fluid dynamic equations based on reduced order models would reduce the computational complexity and limit

the number of computations. These types of models would be more suitable to use in clinical practice due to the shorter computational time.

1.4 Post-processing and Results

The software that solves the fluid dynamics equation would generate the pressure and velocity field over all mesh points (i.e., coronary vessels). These data would need to be processed into an estimation of the virtual FFR to obtain the relevant data and be converted into a report that could be used in clinical practice.

2 ANGIOGRAPHY-BASED FFR

Multiple virtual FFR packages based on angiography have also been developed. All rely on 3D reconstruction and estimates of the simulated flow in the target vessel. The ratio between the simulated flow distally to the stenosis and the simulated flow proximal is the virtual FFR that could be used as an estimate for invasive FFR.

2.1 Technical Development Software Packages

One of the first virtual FFR (vFFR) packages based on rotational invasive angiography images was developed by Morris *et al*[11]. CFD simulations with generic boundary conditions were applied to the reconstructed virtual vessel to calculate a vFFR. A good accuracy (97%) was shown[11, 12]. However, rotational coronary angiography as used for vFFR is less available and more demanding to perform in a clinical setting[12].

Consequently, multiple algorithms have been developed that use the more readily available 3D-QCA based on conventional angiography as input for the dynamic flow computations. Each algorithm uses different parameters, e.g., pressure or Thrombolysis in Myocardial Infarction (TIMI) frame count, and different anatomical settings, e.g., a single or multi-vessel model. An overview of the angiography characteristics, anatomical model, and physiological parameters used in the different algorithms is presented in table 1.

Currently, the most widely evaluated and used angiography-based FFR technique is the quantitative flow ratio (QFR, Medis Medical Imaging Systems, The Netherlands)[13]. The fluid dynamics equations needed to estimate the virtual FFR values would rely on multiple principles and assumptions: 1) coronary pressure would be constant throughout the normal epicardial coronary arteries and would not decrease unless a stenosis was present[13–15], 2) the pressure drop across the lesion would rely on the geometry of the stenosis and the flow moving through the lesion[14], 3) the geometry of the stenosis could be derived from the lumen diameter difference of the stenosis and the reference diameter, an estimation of the diameter size of the healthy lumen, and 4) the coronary flow velocity would be preserved over the length of the vessel, while the mass flow rate (the mass of blood passing per second) would decrease by the presence of the side branches[14]. The combination of these assumptions would require less computational power compared with the CT derived FFR algorithms. The analysis time would mostly depend on the manual selections and adjustments[16]. The QFR software has a CE mark and Agência Nacional de Vigilância Sanitária (ANVISA) clearance for clinical use.

In addition to commercially available QFR, other non-commercially available angiography-based methods to estimate FFR have been developed: 1) the virtual functional assessment index (vFAI) calculates the blood flow in the target vessel needed to assess a simplified virtual resting ratio of the distal coronary pressure to the aortic pressure (Pd/Pa)[12]; 2) Qangio software reconstructs a virtual target lesion and applies a classic simplified fluid dynamic equation to estimate the pressure gradients. This would incorporate the actual flow velocity by the TIMI frame count method to enable the fast estimation of the pressure gradient[17]; and 3) the FFRangio algorithm (CathWorks Ltd., Israël) uses individually tuned boundary conditions derived from the angiographic anatomy, the heart rate, and blood pressure[18, 19]. Using these boundaries, coronary flow under maximal hyperemia would be computed from which the FFRangio values could be estimated. Other available algorithms use the Cardiovascular Angiographic Analysis System (CAAS) to reconstruct the coronary tree; namely, CAAS-vFFR (Pie Medical Imaging, The Netherlands) and quantitative coronary angiography-derived translesional pressure (QCA-TP)[9, 20]. Furthermore, advancements on supervised deep learning neural network to calculate a virtual FFR were made[21].

2.2 Validation of the Software Packages

Angiography-based virtual FFR has been validated in multiple studies mostly against invasive FFR. The first prospective observational multicenter study, the FAVOR pilot study aimed to evaluate the QFR to invasive FFR[14]. A good accuracy (accuracy of 86%) for identifying significant coronary artery disease (CAD) defined as FFR of ≤0.80 was reported[14, 22]. The FAVOR Ⅱ China study was the first adequately powered study to assess the diagnostic performance of the QFR in 308 patients[8]. The QFR analysis had an accuracy of 92.7% and therefore met the pre-specified accuracy target value of 75%[8]. The FAVOR Ⅱ Europe-Japan study showed superior sensitivity (86.5%) and specificity (86.9%) of the QFR compared with the 2D-QCA in 272 patients[23]. The accuracy observed in this study was slightly lower than in the FAVOR Ⅱ China study (86.8% *versus* 92.7%), which might be explained by the higher percentage of lesions with FFR values around the cut-off point in the former study[8, 23]. A third prospective

Table 1 Overview of the angiography characteristics, anatomical model, and physiological parameters used in the different algorithms

	QFR[8, 13, 14, 23, 24]	vFFR[11]	CAAS vFFR[9]	CAAS QCA-TP[20]	FFRangio[19]	vFAI[12]
Clinical imaging						
Imaging requirements	Monoplane projections Frame rate of at least 12.5 fps 5F catheter	Single axis rotational coronary angiography 6F catheter	Monoplane angiographic projections	Monoplane projections 4F to 6F coronary catheters	Frame rate of 10–15 images/s 6F diagnostic catheters	Monoplane or biplane projections
Acquisitions	Two projections with anangle difference ≥25 degrees; 3 full cardiac cycles	Two clear projections from similar phases of the cardiac cycle as close to 90° apart	Two projections with an angle difference ≥30 degrees	One angiographic view with the least foreshortening	Two projections with an angle difference ≥30 degrees	Two projections with an angle difference ≥30 degrees
Hyperemia needed	Non-compulsory; adenosine	No	No	No	No	No
Anatomical model						
How is it generated?	Semi-automated contour detection using 3D QCA with manual adjustments	3D-image segmentation using a Philips 3D workstation	Semi-automated contour detection using CAAS Workstation 8.0, with manual adjustments	Semi-automated contour detection using CAAS Ⅱ QCA-2D system	Semi-automated contour detection using Siemens Syngo IZ3D (based on CAAS QCA-3D)	Semi-automated contour detection using CAAS QCA-3D system
Mathematical model						
Flow rate	Volumetric flow rate was calculated by the TIMI frame count using the lumen volume of the reconstructed coronary tree divided by the mean transport time	The inlets and outlets were defined according to the position from which the physiological data were recorded. Measured pressure and derived flow data were imported, processed, and applied to the inlet and outlets as boundary conditions, and a definition file was created that fully specified the arterial model for the CFD solver. Windkessel models were used to determine the resistance and compliance values to produce a generic value applicable to the whole cohort	The pressure drop was calculated instantaneously by applying physical laws, including viscous resistance and separation loss effects present in the coronary flow behavior. The pressure drop calculation by CAAS vFFR included the patient's specific aortic pressure. Maximum hyperemic blood flow was empirically determined from the clinical data	The calculated pressure gradient (ΔP) across a stenosis was defined as: $\Delta P=FV+SV^2$. F: the coefficient of pressure loss due to viscous friction S: the coefficient of pressure loss due to exit separation (flow separation). The intersection of the curve (100-ΔP), with coronary perfusion pressure under the hyperemia line was the QCA-TP estimate	Non-stenotic segments: A reduced-order model was used in combination with a lumped parameter model of the coronary microvasculature Stenotic/bifurcation segments: Reduced-order pressure drop models were used incorporating the complex shape of the stenosis. Pressure drop models were coupled with the reduced-order model for the remaining vasculature. The mean aortic pressure and heart rate, the vessel cross section of the non-diseased proximal segment of the modeled coronary vessel, Murray's law to distribute assumed flow over more than one outlet, estimates of coronary microvascular resistance were used to determine the flow at rest	Blood was treated as dynamic viscosity of 0.0035 Pa·s and having a density of 1050 kg/m^3
Outlet conditions	Outflow, fully developed flow, and condition were applied at the outlets Finite volume method with the element size between 0.02 mm and 0.2 mm automatically adapted to the complexity of the local anatomy and parallel computing were used					Steady flow, fully developed, was specified as the boundary condition at the outlet (1 mL/s and 3 mL/s)
Inlet conditions	The mean hyperemic volumetric flow rate and the mean pressure at the guiding catheter tip were applied at the inlet					A reference pressure of 100 mmHg (the average aortic pressure in humans) was imposed at the inlet.
Fluid assumptions	Blood modeled as Newtonian fluid	No assumptions made	No assumptions made	No assumptions made	Blood modeled as Newtonian fluid	Blood modeled as Newtonian fluid

(Continued to the next page)

(Continued from the last page)

	QFR[8, 13, 14, 23, 24]	vFFR[11]	CAAS vFFR[9]	CAAS QCA-TP[20]	FFRangio[19]	vFAI[12]
Practical considerations						
Operator	Users need to be trained, certified, and follow the standard operating procedure	Not specified	Not specified	Not specified	Not specified	Not specified
Computational requirements	Standard desktop computer	High-end workstation required due to the computationally intensive process	Not specified			
Time	4.36±2.55 min	Approximately 24 h	Not assessed			

CAAS: Cardiovascular Angiographic Analysis System; CFD: computational fluid dynamics; F: French; QCA: quantitative coronary angiography; QCA-TP: quantitative coronary angiography derived translesional pressure; QFR: quantitative flow ratio; TIMI: thrombolysis in myocardial infarction; vFAI: virtual functional assessment index; vFFR: virtual fractional flow reserve

study, WIFI Ⅱ, evaluated the diagnostic performance and feasibility of the QFR in 172 unselected consecutive patients as part of the Dan-NICAD study[23]. A sensitivity of 77%, a specificity of 86% and an accuracy of 83% were reported, which were lower than those observed in the FAVOR studies. Possible explanations could be found in the stricter inclusion criteria of the FAVOR studies and the intention to exclude only the cases suffering from extremely poor angiographic quality in the WIFI study[8, 14, 24]. Moreover, the QFR analyses in the FAVOR pilot and FAVOR Ⅱ China studies were performed by a highly trained core lab, which might have also contributed to the observed differences[8, 14, 24]. Multiple observational studies were also performed and observed similar diagnostic results as described in the FAVOR studies and WIFI Ⅱ[13, 15, 16, 25–27]. An overview of the study characteristics and results is given in table 2.

The QFR would require some user interaction, such as frame selection, selection of anatomical landmarks, indicating the start and endpoint of the target vessel, lumen contouring, deciding on the reference contours of the vessel, and contrast flow evaluation, which might affect the repeatability between observers[23, 27–29]. The reproducibility of the QFR has been assessed in four studies and all found good agreement between the observers (mean difference: 0.02±0.04[28], 0.004±0.03[26], –0.01±0.06[23], and 0.01±0.08[29]). No systematic error of the QFR between the observers was found, and no differences in the performance of the QFR for the low and high FFR values were reported. When using the same standardized operating procedure, the QFR measurements seemed to be robust and reproducible. However, some remarks could be made. All studies except one[29] were performed that focused on the measures of agreement—how close are the scores for the repeated measurements?—and not on measurements of reliability—how well can patients be distinguished from each other[23, 28, 30]? Reproducibility was assessed by means of the Pearson correlation coefficient, which was not the most optimal measurement since the measurements could be perfectly correlated (r=1) even if the agreement and reliability were poor due to (systematic) measurement errors.

2.3 Clinical Implications

In light of its diagnostic performance and reliability, angiography-based FFR has some advantages over FFR. First, the QFR would require less evaluation time than FFR (5 min *versus* 7 min[23]) and could be easily implemented since data acquisition would minimally disrupt the routine angiography. Second, the discomfort of patients caused by adenosine-induced hyperemia could be prevented and it might therefore result in less side effects and improve patient safety. Finally, besides the improvements of the diagnostic workflow and patient care, the use of angiography-based FFR might

Table 2 Overview of the published study characteristics and results

	Tu 2014	Tu 2016	Xu 2017	Yazaki 2017	Emori 2018	Koltowski 2018	Smit 2018	Ties 2018	Westra 2018	Westra 2018	Stähli 2019
Trial name		Favor pilot	FAVOR Ⅱ China						FAVOR Ⅱ E-J	WIFI Ⅱ	
Type	QFR	QFR	QFR	QFR	QFR	QFR	QFR	QFR	QFR	QFR	QFR
Population characteristics (*n*)	68	73	308	142	100	268	290	96	272	172	436
Male gender	47 (69.1)	61 (83.5)	227 (73.7)	100 (70.4)	71 (71)	193 (72)	201 (69.3)	58 (60.4)	196 (72)	116 (67)	296 (68)
Age (years)	62.0±9.0	65.8±8.9	61.3±10.4	72.5±9.5	70±0	66.3±9.98	66.5±9.4	63.9±10.3	67±10	61±8	71.5 (63.0–77.0)
BMI	27.5 (24.8–30.8)	26.3±6.3	25.2±3.3	23.9±3.2	–	–	–	27.3±5.1	27±5	27±4	26.0 (23.9–29.2)
Dyslipidemia	52 (76.5)	–	139 (45.1)	88 (62.0)	58 (58)	146 (54.5)	–	70 (72.9)	188 (68)	–	345 (79)
Hypertension	47 (69.1)	32 (43.8)	185 (60.1)	101 (71.1)	73 (73)	203 (75.7)	208 (74.3)	68 (70.8)	201 (74)	121 (70)	383 (88)
Diabetes mellitus	20 (29.4)	17 (27.4)	86 (27.9)	41 (28.9)	48 (48)	75 (28)	67 (23.8)	24 (25.0)	78 (29)	18 (10)	98 (23)
Current smoker	16 (23.5)	–	87 (28.2)	33 (23.2)	21 (21)	28 (10.4)	–	26 (28.6)	156 (57)***	101 (59)***	148 (34)***
Family history of CAD	–	–	51 (16.6)	–	–	28 (10.4)	–	42 (46.2)	73 (27)	69 (40)	62 (14)
Vessel characteristics (*n*)	77	84	332	151	100	306	334	101	317	255	516
LAD	49 (63.6)	46 (54.8)	185 (55.7)	96 (63.6)	63 (63)	174 (56.9)	225 (67.4)	67 (66.3)	160 (50)	129 (51)	287 (56)
LCx	13 (16.9)	12 (14.3)	49 (14.8)	25 (16.6)	23 (23)	31 (10.1)	48 (14.4)	15 (14.9)	50 (16)	29 (11)	67 (13)
RCA	13 (16.9)	19 (22.6)	87 (26.2)	26 (17.2)	14 (14)	81 (26.5)	33 (9.9)	19 (18.8)	68 (22)	46 (18)	119 (23)
Other	2 (2.6)	7 (8.3)	11 (3.4)	4 (2.7)	0 (0)	20 (6.5)	28 (8.4)		39 (12)	51 (20)	43 (8)
FFR	0.84 (0.78–0.89)	0.85 (0.77–0.89)	0.82±0.12	0.85 (0.79–0.92)	0.75±0.10	0.81 (0.73–0.87)	0.85±0.08	0.88 (0.82–0.92)	0.83±0.09	0.85 (0.77–0.90)	0.88 (0.82–0.92)
FFR ≤0.80	23 (29.9)	27 (32.1)	113 (34.2)	46 (30.5)	69 (69)	130 (42.5)	–	21	104 (33)	86 (36)	100 (19)
Diagnostic measure	cQFR	cQFR									
Accuracy (%)	88	86	93	89	94	85	86	90	87	83	93
Sensitivity (%)	78	74	95	89	97	84	70	67	87	77	75
Specificity (%)	93	91	92	89	87	87	92	96	87	86	98
PPV (%)	82	80	86	77	94	82	77	82	76	75	89
NPV (%)	91	88	97	95	93	88	89	92	93	87	94
AUC	0.93	0.92	0.96	0.93	–	0.94	0.92	0.92	0.92	0.86	0.86
Correlation coefficient	0.81	0.77	0.86	0.80	0.89	0.85	0.81	0.70	0.83	0.70	0.82
Mean difference	0.00±0.06	0.001±0.059	–0.01±0.063	0.01±0.05	–0.01±0.07	0.002±0.054	0.01±0.051	–0.001±0.06	0.01±0.06	0.01±0.08	0.01±0.07

(Continued to the next page)

(Continued from the last page)

	Tar 2018	Masdjedi 2019	Morris 2013	Trobs 2016	Pellicano 2017	Fearon 2019	Omori 2019	Li 2020	Papafaklis 2014	Seike 2016		
Trial name		FAST	VIRTU-1					FLASH FFR				
Type	Own software	CAAS vFFR	vFFR	FFRangio	FFRangio	FFRangio	FFRangio	caFFR	vFAI	QCA-TP		
Population characteristics (*n*)	64	100	19	73	184	301	50	323	120	132		
Male gender	42 (65.5)	67 (67)	12 (63)	48 (66)	123 (67)	223 (74)	36 (72)	213 (65)	87 (72.5)	92 (70)		
Age (years)	62±9.8	64±11	64 (45–81)	67±11	65.9±9.5	64.7±9.7	72.5±9.1	63.2±9.4	64.0±9.6	70.0±10.2		
BMI	NA	28±5	29	27.7±2.9	–	28.9±4.8	23.6±3.2	25.5±3.3	–	23.9±3.5		
Dyslipidemia	57 (89.1)	59 (59)	19 (100)	71 (97)	164 (89)	230 (76)	33 (66)	146 (45)	78 (65)	84 (64)		
Hypertension	51 (79.7)	70 (70)	16 (84)	64 (88)	124 (67)	208 (69)	37 (74)	215 (66)	70 (58.3)	87 (66)		
Diabetes mellitus	17 (26.6)	26 (26)	1 (5)	17 (23)	59 (32)	96 (32)	13 (26)	101 (31)	34 (28.3)	54 (41)		
Current smoker	18 (28.1)	25 (25)	4 (21)	11 (15)	32 (17)	159 (53)***	10 (20)	85 (26)	33 (27.6)	27 (20)		
Family history of CVD	–	–	–	27(27)	60 (33)	116 (39)	5 (10)		–			
Vessel characteristics (*n*)	68	100	22	100	203	319	118	323	139	152		
LAD	44	60 (60)	10 (45.5)	46 (46)	118 (58)	173 (54)	51 (43)	195 (60)	90 (64.7)	98 (64)		
LCx	18	13 (13)	1 (4.5)	23 (23)	30 (15)	61 (19)	43 (36)	36 (11)	19 (13.7)	28 (18)		
RCA	6	27 (27)	10 (45.5)	31 (31)	39 (19)	77 (24)	24 (20)	87 (27)	30 (21.6)	26 (17)		
Other	0	0 (0)	1 (4.5)	0 (0)	16 (8)	8 (3)	0 (0)	10 (3)	0 (0)	0 (0)		
FFR		0.82±0.08		0.84±0.1		0.81±0.13	0.83±0.12	0.83±0.09	0.84 [0.75–0.90]	0.76±0.14		
FFR ≤0.80		NA	10 (45.5)	29 (29)		138 (43)		107 (33)	52 (37)	83 (54)		
Diagnostic measure										LAD (≤0.728)	LCx (≤0.605)	RCA (≤0.644)
Accuracy (%)		–	97	90	93	92	92	96	88	87	89	89
Sensitivity (%)	100	–	86	79	88	94	92	90	90	89	93	92
Specificity (%)	90	–	100	94	95	91	92	99	86	84	85	85
PPV (%)	88	–	100	85	–	89		97	80	87	88	86
NPV (%)	100	–	97	92	–	95		95	94	86	92	92
AUC	0.96	0.93	–	0.93	0.99; 0.96; 0.90	0.94	0.92	0.98	0.92	0.93	0.88	0.94
Correlation coefficient	0.86	0.89	0.84	0.85	0.88	0.80	0.83	0.89	0.78	0.78	0.78	0.84
Mean difference	–0.01±0.08	0.01±0.0356	0.02±0.09	0.008±0.06	0.007±0.05	–0.01±0.13	0.017±0.07	–0.02±0.096	–0.0039±0.085	–	–	–

AUC: area under the curve; BMI: body mass index; CAAS: cardiovascular angiographic analysis system; CAD: coronary artery disease; CVD: cardiovascular diseases; FFR: fractional flow reserve; LAD: left anterior descending artery; LCx: left circumflex artery; NPV: negative predictive value; PPV: positive predictive value; QCA-TP: quantitative coronary angiography derived translesional pressure; QFR: quantitative flow ratio; RCA: right coronary artery; vFAI: virtual functional assessment index, vFFR: virtual fractional flow reserve. ***Current and past smokers

reduce the healthcare costs. As such, the angiography-based FFR strategy would have the potential of a wider adoption of FFR guided lesion assessment[14].

To use angiography-based FFR for clinical decision-making, variation in agreement, especially close to the threshold of 0.80, the so-called grey zone, between angiography-based FFR and FFR should be considered. Hybrid strategies, in which angiography-based FFR combined with invasive FFR for lesions in the "grey zone", were proposed to optimize the diagnostic accuracy. Multiple thresholds for the grey zone were proposed for the QFR: the QFR-treat values between 0.75–0.78 to the QFR-defer values between 0.85–0.87[15, 23, 24, 26]. In the WIFI study, the FFR assessment could have been avoided in 68% when using the hybrid strategy[24]. Similar results were reported from the FAVOR Ⅱ Europe-Japan where a grey zone would have saved the pressure wires and adenosine in 64% of the lesions[23]. Moreover, hospitals not capable of performing FFR could use angiography-based FFR as gatekeeper for referrals to the hospitals where FFR and PCI could be performed. Currently, these hospitals assess the severity of the lesions visually although visual assessment alone is known to be inaccurate for the assessment of functional significant CAD[26, 31]. Additionally, Smit *et al* showed in their study that a 50% reduction in referrals for FFR and PCI could be obtained based on a QFR threshold of 0.86, while 5% of the patients were classified as false negative and 7.5% as false positive[26].

The first randomized trial on the impact of the QFR on the clinical endpoints was the FAVOR Ⅲ China (NCT03656848)[32]. In this study, a QFR-guided strategy was compared to a standard angiography guided strategy for lesion selection for the PCI on major cardiovascular events in 3825 patients. It could be concluded that the lesion selection for the PCI using QFR guidance improved the clinical outcomes at one year by reducing the procedural complications. QFR guidance would improve the long-term results compared with the standard angiography guided PCI. However, wire-based FFR was not allowed and therefore the trial procedure deviated from the clinical practice.

Following the diagnostic performance assessment of angiography-based FFR in well-defined standardized populations, angiography-based FFR computations were applied in different patient settings. Emori *et al* performed a retrospective study in which they assessed the performance of the QFR in prior MI-related coronary arteries[33]. A mismatch between visually assessed diameter stenosis and FFR was often observed[31]. The accuracy of the QFR was reduced in prior-MI related arteries compared with non-prior MI related lesions, which suggested that QFR was less useful for the assessment of hemodynamically significant stenosis in prior-MI vessels[33]. The QFR was also evaluated for non-culprit lesions in ST-segment elevation myocardial infarction (STEMI) patients by Spitaleri *et al*[34]. Good reproducibility [r=0.98 and mean difference of 0.004 (–0.027–0.34)] and diagnostic performance (sensitivity: 88%, specificity: 97%, and accuracy: 94%) of the QFR were demonstrated in the NCLs when using invasive FFR as a reference[34]. The performance of QFR was also evaluated prior to transcatheter aortic valve implantation (TAVI) in patients with severe aortic stenosis. Pre-TAVI QFR had a good diagnostic performance using post-TAVI FFR as a reference; however, the results should be interpreted with caution because of the limited sample size (n=28)[35]. Likewise, Mejía-Rentería *et al* assessed the diagnostic performance of the QFR in the presence of coronary microcirculatory dysfunction (CMD)[36]. CMD, although hardly evaluated, was acknowledged as a component of ischemic heart disease. The impact of CMD on FFR and QFR has been underreported. Mejía-Rentería *et al* used the index of microcirculatory resistance (IMR) to describe CMD. They reported a lower positive predictive value of the QFR in the CMD subgroup. Nevertheless, even in the presence of a high IMR, the QFR remained superior to visual assessment by angiography alone in diagnosing hemodynamically significant CAD[36]. Furthermore, no differences were found in the diagnostic performance in diabetic patients often suffering from CMD[37].

2.4 Challenges

Some challenges and limitations need to be kept in mind when using the angiography-based FFR. First, invasive FFR is used as a reference standard to determine the diagnostic accuracy of angiography-based FFR since it is the best reference test for hemodynamically significant CAD. However, FFR is a surrogate for the coronary blood flow, thus inferring that angiography-based FFR is a surrogate of a surrogate. Secondly, most of the performed studies suffered from selection bias. Patients with (severe) co-morbidities were excluded as well as those with lesions in the vein grafts, stents, or bifurcations, which could result in an overestimation of the diagnostic performance. Moreover, all studies performed to date have been observational studies. No randomized controlled trials (RCT) comparing clinical endpoints, such as major adverse cardiovascular events (MACE) between the standard strategy, including FFR (FAVOR Ⅲ China) and the angiography-based FFR strategy have been performed yet. In addition to the induced selection bias, the exclusion criteria as mentioned before limited the generalizability of the diagnostic value. Thirdly, the accuracy of angiography-based FFR would strongly depend on the quality of the imaging. Although dedicated acquisition guidelines were applied in most studies, potentially suboptimal imaging quality due to the low frame acquisition speed,

overlapping vessels, foreshortening, moderate contrast filling, or briskness of the contrast injection could not be avoided[27]. The impact of the variation in the quality of the imaging on the diagnostic performance of angiography-based FFR has not been assessed. Moreover, angiography-based FFR analysis would involve user interactions that would require training of the operators. Fourth, angiography-based FFR would strongly depend on the difference between the reference diameter and the minimal luminal diameter. Limited availability of disease-free segments, both proximal and distal of the lesion, would complicate the estimation of the reference diameter[14]. Eccentric lesions might also affect the degree of the stenosis diameter or the reference diameter and influence the accuracy in these kinds of lesions[38]. This could affect the revascularization decision for the eccentric lesions. Additionally, QCA would underestimate the stenosis diameter and stent length in the stented vessels. Fifth, the side branches of the bifurcation lesions (Medina type 1,1,1 or 1,0,1) could not be evaluated with high accuracy[27]. The impact of bifurcation on the coronary flow velocity and distribution is unknown. Moreover, attainment of adequate imaging quality could be challenging due to the overlapping vessels. Sixth, microcirculatory resistance would represent a major challenge and scientific limitation in angiography-based FFR. The angiography-based FFR models used fixed boundary conditions for the microcirculatory resistance, whereas the invasive FFR measurements were affected by the differences in this resistance. Variations in microcirculatory resistance could also limit the increase in the blood flow after vasodilatation and limit the corresponding pressure drop distal to the lesion. Therefore, the severity of the stenosis could be underestimated if the microcirculatory resistance was high, mainly in patients with prior myocardial infarction and diabetes complicated with the left ventricular hypertrophy[36, 39]. Last of all, the different algorithms described in this review were not directly compared.

2.5 Ongoing Trials and Perspective

As previously mentioned, no RCT comparing the clinical outcomes, such as MACE between the standard strategy and the angiography-based FFR strategy has been performed to date. Moreover, no information is available on the cost-effectiveness of the angiography-based FFR strategies. Currently, two clinical trials are recruiting. The first multicenter RCT, the FAVOR Ⅲ Europe-Japan (NCT03729739) would investigate if a QFR-guided strategy is non-inferior to standard invasive FFR-guided strategy in terms of MACE after 12 months. Although this trial would allow for functional testing, the cost-effectiveness would not be assessed. The primary completion date was expected in June 2021, and the estimated sample size was 2000 patients at high risk of having at least one coronary stenosis. In addition to the aforementioned studies, the RCTs on the added value of the QFR prior to coronary artery bypass grafting (CABG) and primary valve surgery were proposed. The Clinical Effect of QFR-guided Coronary Artery Bypass Grafting: A Randomized Controlled Trial (NCT03770520) investigated the clinical value of the QFR in eligible patients undergoing CABG. A total of 208 patients were randomized to QFR-guided or angiography-guided heart team discussion, and the success was evaluated based on the one-year graft patency. The estimated completion of the study was in August 2020. A second trial was planned on the QFR prior to CABG, The Clinical Effect of QFR-guided Coronary Artery Bypass Grafting: A Randomized Controlled Trial (NCT03770520). This study randomized 208 patients between CABG surgery based on the ICA and QFR, and CABG surgery based on the heart team discussion of the ICA to investigate if the QFR could be adopted in CABG-planning with the results in better graft patency and less MACE at one year. The estimated primary completion date was August 2020. The Angio-based Quantitative Flow Ratio Virtual PCI *Versus* Conventional Angio-guided PCI in the Achievement of an Optimal Post-PCI QFR (NCT04664140) trial assessed the effect of procedural planning based on the QFR on the rate of patients with a post-PCI optimal functional result compared to ICA guided PCI in 300 patients. The effect of the post-PCI was evaluated with the QFR, and an optimal result was defined as the proportion of the patients with a final post-PCI QFR result ≥0.90. The expected primary completion date was June 2021. Last of all, the FAVOR IV-QVAS (NCT03977129) evaluated the effectiveness of QFR-guided revascularization compared to angiography-guided revascularization in patients planned for primary valvular surgery and comorbid CAD with the diameter stenosis of ≥50%. The effectiveness was assessed in 792 patients and was defined as a composite outcome, including all-cause death, non-fatal myocardial infarction, non-fatal stroke, unplanned coronary revascularization, and new renal failure requiring dialysis within 30 days after valvular surgery.

3 CONCLUSION

New less-invasive techniques as the QFR have been developed to overcome the burden of FFR and could obviate the need for the additional flow or pressure wires. The diagnostic performance of angiography-based FFR has been well studied in both prospective and retrospective studies although the information on the clinical outcomes and cost-effectiveness is still lacking. Further randomized studies would be required, and the RCTs outlined above would add to what is

currently known.

Conflict of Interest Statement

Nothing to disclose.

REFERENCES

1 Toth G, Hamilos M, Pyxaras S, *et al*. Evolving concepts of angiogram: Fractional flow reserve discordances in 4000 coronary stenoses. Eur Heart J, 2014,35(40):2831-2838

2 Pijls NHJ, Fearon WF, Tonino PAL, *et al*. Fractional flow reserve versus angiography for guiding percutaneous coronary intervention in patients with multivessel coronary artery disease: 2-Year follow-up of the FAME (fractional flow reserve versus angiography for multivessel evaluation) study. J Am Coll Cardiol, 2010,56(3):177-184

3 Dattilo PB, Prasad A, Honeycutt E, *et al*. Contemporary Patterns of Fractional Flow Reserve and Intravascular Ultrasound Use Among Patients Undergoing Percutaneous Coronary Intervention in the United States Insights From the National Cardiovascular Data Registry. J Am Coll Cardiol, 2012,60(22):2337-2339

4 Parikh RV, Liu G, Plomondon ME, *et al*. Utilization and Outcomes of Measuring Fractional Flow Reserve in Patients With Stable Ischemic Heart Disease. J Am Coll Cardiol, 2020,75(4):409-419

5 Tebaldi M, Biscaglia S, Pecoraro A, *et al*. Fractional flow reserve implementation in daily clinical practice: A European survey. Int J Cardiol, 2016,207:206-207

6 Hannawi B, Lam WW, Wang S, *et al*. Current use of fractional flow reserve: A nationwide survey. Tex Heart Inst J, 2014,41(6):579-584

7 Taylor CA, Fonte TA, Min JK. Computational fluid dynamics applied to cardiac computed tomography for noninvasive quantification of fractional flow reserve: scientific basis. J Am Coll Cardiol, 2013,61(22):2233-2241

8 Xu B, Tu S, Qiao S, *et al*. Diagnostic Accuracy of Angiography-Based Quantitative Flow Ratio Measurements for Online Assessment of Coronary Stenosis. J Am Coll Cardiol, 2017,70(25):3077-3087

9 Masdjedi K, Zandvoort L van, Balbi MM, *et al*. Validation of 3-Dimensional Quantitative Coronary Angiography based software to calculate Fractional Flow Reserve: Fast Assessment of Stenosis severity (FAST)-study. EuroIntervention, 2020,16(7):591-599

10 Tu S, Westra J, Adjedj J, *et al*. Fractional flow reserve in clinical practice: From wire-based invasive measurement to image-based computation. Eur Heart J, 2020,41(34):3271-3279,

11 Morris PD, Ryan D, Morton AC, *et al*. Virtual fractional flow reserve from coronary angiography: Modeling the significance of coronary lesions. Results from the VIRTU-1 (VIRTUal fractional flow reserve from coronary angiography) study. JACC Cardiovasc Interv, 2013,6(2):149-157

12 Papafaklis MI, Muramatsu T, Ishibashi Y, *et al*. Fast virtual functional assessment of intermediate coronary lesions using routine angiographic data and blood flow simulation in humans: Comparison with pressure wire – fractional flow reserve. EuroIntervention, 2014,10(5):574-583

13 Tu S, Barbato E, Köszegi Z, *et al*. Fractional Flow Reserve Calculation From 3-Dimensional Quantitative Coronary Angiography and TIMI Frame Count. JACC Cardiovasc Interv, 2014,7(7):768-777

14 Tu S, Westra J, Yang J, *et al*. Diagnostic Accuracy of Fast Computational Approaches to Derive Fractional Flow Reserve From Diagnostic Coronary Angiography. JACC Cardiovasc Interv, 2016,9(19):2024-2035

15 Yazaki K, Otsuka M, Kataoka S, *et al*. Applicability of 3-Dimensional Quantitative Coronary Angiography-Derived Computed Fractional Flow Reserve for Intermediate Coronary Stenosis. Circ J, 2017,81(7):988-992

16 Kołtowski Ł, Zaleska M, Maksym J, *et al*. Quantitative flow ratio derived from diagnostic coronary angiography in assessment of patients with intermediate coronary stenosis: a wire-free fractional flow reserve study. Clin Res Cardiol, 2018,107(9):858-867

17 Tar B, Jenei C, Dezsi CA, *et al*. Less invasive fractional flow reserve measurement from 3-dimensional quantitative coronary angiography and classic fluid dynamic equations. EuroIntervention, 2018, 14(8):942-950

18 Pellicano M, Lavi I, De Bruyne B, *et al*. Validation study of image-based fractional flow reserve during coronary angiography. Circ Cardiovasc Interv, 2017,10(9):e005259

19 Tröbs M, Achenbach S, Röther J, *et al*. Comparison of Fractional Flow Reserve Based on Computational Fluid Dynamics Modeling Using Coronary Angiographic Vessel Morphology Versus Invasively Measured Fractional Flow Reserve. Am J Cardiol, 2016,117(1):29-35

20 Seike F, Uetani T, Nishimura K, *et al*. Correlation Between Quantitative Angiography–Derived Translesional Pressure and Fractional Flow Reserve. Am J Cardiol, 2016,118(8):1158-1163

21 Huang FY, Liu Q, Liu XX, *et al*. Virtual fractional flow reserve and virtual coronary stent guided percutaneous coronary intervention. Cardiol J, 2020,27(3):318-319

22 Knuuti J, Wijns W, Saraste A, *et al*. 2019 ESC Guidelines for the diagnosis and management of chronic coronary syndromes. Eur Heart J, 2020,41(3):407-477

23 Westra J, Andersen BK, Campo G, *et al*. Diagnostic performance of in-procedure angiography-derived quantitative flow reserve compared to pressure-derived fractional flow reserve: The FAVOR Ⅱ Europe-Japan study. J Am Heart Assoc, 2018,7(14):e009603
24 Westra J, Tu S, Winther S, *et al*. Evaluation of Coronary Artery Stenosis by Quantitative Flow Ratio during Invasive Coronary Angiography: The WIFI Ⅱ Study (Wire-Free Functional Imaging Ⅱ). Circ Cardiovasc Imaging, 2018,11(3):e007107
25 Emori H, Kubo T, Kameyama T, *et al*. Quantitative flow ratio and instantaneous wave-free ratio for the assessment of the functional severity of intermediate coronary artery stenosis. Coron Artery Dis, 2018,29(8):611-617
26 Smit JM, Koning G, Van Rosendael AR, *et al*. Referral of patients for fractional flow reserve using quantitative flow ratio. Eur Heart J Cardiovasc Imaging, 2019,20(11):1231-1238
27 Ties D, van Dijk R, Pundziute G, *et al*. Computational quantitative flow ratio to assess functional severity of coronary artery stenosis. Int J Cardiol, 2018,271:36-41
28 van Rosendael AR, Koning G, Dimitriu-Leen AC, *et al*. Accuracy and reproducibility of fast fractional flow reserve computation from invasive coronary angiography. Int J Cardiovasc Imaging, 2017,33(9):1305-1312
29 Westra J, Sejr-Hansen M, Koltowski L, *et al*. Reproducibility of quantitative flow ratio: The QREP study. EuroIntervention, 2022,17(15):1252-1259
30 Chang Y, Chen L, Westra J, *et al*. Reproducibility of quantitative flow ratio: An inter-core laboratory variability study. Cardiol J, 2020,27(3):230-237
31 Park SJ, Kang SJ, Ahn JM, *et al*. Visual-Functional Mismatch Between Coronary Angiography and Fractional Flow Reserve. Int J Angiol, 2016,25(4):229-234
32 Xu B, Tu L, Song L, *et al*. Angiographic quantitative flow ratio-guided coronary intervention (FAVOR Ⅲ China): a multicentre, randomised, sham-controlled trial. Lancet, 2021,398 (10317):2149-2159
33 Emori H, Kubo T, Kameyama T, *et al*. Diagnostic Accuracy of Quantitative Flow Ratio for Assessing Myocardial Ischemia in Prior Myocardial Infarction. Circ J, 2018,82(3):807-814
34 Spitaleri G, Tebaldi M, Biscaglia S, *et al*. Quantitative Flow Ratio Identifies Nonculprit Coronary Lesions Requiring Revascularization in Patients with ST-Segment-Elevation Myocardial Infarction and Multivessel Disease. Circ Cardiovasc Interv, 2018,11(2):1-10
35 Sejr-Hansen M, Høj Christiansen E, Ahmad Y, *et al*. Performance of quantitative flow ratio in patients with aortic stenosis undergoing transcatheter aortic valve implantation. Catheter Cardiovasc Interv, 2022,99(1):68-73
36 Mejía-Rentería H, Lee JM, Lauri F, *et al*. Influence of Microcirculatory Dysfunction on Angiography-Based Functional Assessment of Coronary Stenoses. JACC Cardiovasc Interv, 2018,11(8):741-753
37 Smit JM, El Mahdiui M, van Rosendael AR, *et al*. Comparison of Diagnostic Performance of Quantitative Flow Ratio in Patients With Versus Without Diabetes Mellitus. Am J Cardiol, 2019,123(10):1722-1728
38 Takashima H, Waseda K, Gosho M, *et al*. Severity of morphological lesion complexity affects fractional flow reserve in intermediate coronary stenosis. J Cardiol, 2015,66(3):239-245
39 Morris PD, Ryan D, Morton AC, *et al*. Virtual Fractional Flow Reserve From Coronary Angiography: Modeling the Significance of Coronary Lesions. JACC Cardiovasc Interv, 2013,6(2):149-157

(Received June 21, 2021; accepted May 30, 2022)